

Causal motifs and existence of endogenous cascades in directed networks with application to company defaults

Irena Barjašić,¹ Hrvoje Štefančić,² Vedrana Pribičević,^{3, 4} and Vinko Zlatić⁵

¹*Faculty of Science, University of Zagreb, 10000 Zagreb, Croatia,*

²*Catholic University of Croatia, Ilica 242, 10000 Zagreb, Croatia*

³*Zagreb School of Economics and Management, Zagreb, Croatia*

⁴*Faculty of Economics, University of Ljubljana, Ljubljana, Slovenia*

⁵*Division of Theoretical Physics, Ruder Bošković Institute, Zagreb, Croatia*

(Dated: June 15, 2022)

Motivated by detection of cascades of defaults in economy, we developed a detection framework for endogenous spreading based on causal motifs we define in this paper. We assume that vertex change of state can be triggered by endogenous or exogenous event, that underlying network is directed and that times when vertices changed their states are available. In addition to data of company defaults we use, we simulate cascades driven by different stochastic processes on different synthetic networks. We also extended an approximate master equation method to directed networks with temporal stamps in order to understand in which cases detection is possible. We show that some of the smallest motifs can robustly detect cascades.

I. INTRODUCTION

Stochastic cellular automaton and Interacting particle systems belong to most ubiquitous models of dynamics on different complex systems. They are used to model epidemics [1–3], systemic risk in financial industry [4, 5], propagation of information in society [6], queuing [7] etc. In some of these systems, dynamics can lead to the formation of cascades like, for example, a fast evolving contagion or a series of company defaults. Detecting such events can be very important as is the case in new previously unknown pathogen or for understanding what drives some default avalanche in economy.

Not all the data for the investigated system are necessarily available. Contact data are of paramount importance to understand which pathways a new pathogen [8, 9] takes or what is the reason for companies default [10]. Lacking this data, researchers can often reconstruct only a portion of the network to model the spreading processes. Often, when the ideal data of the real system would be most precisely represented as a multiplex network [11–13], available data enables reconstruction of only one or two layers. In some other cases there really is no network effect in spreading: like for example, when a person surviving an earthquake is tweeting about it. Appropriate physical model for such a correlated event would be influence of external field on the system, as earthquake is a “field effect” that all the vertices (people) at certain geographic area experience similarly. Not knowing the layers that are not present in the available data also suggests that modeling spread influenced by these real layers is best done as a field effect in the data at hand.

Question that arises is, whether the observed dynamics in the data can be explained through stochas-

tic cellular automata on the network that is available - therefore being endogenous with respect to the data, or it would be more appropriate to model it as an purely exogenous (field effect) influence.

Motivation for this research is directly related to economics, more concretely - a problem of default cascades [14, 15]. Knowing what causes companies to go into default is crucial for every economy. When a company fails to repay a debt, it is said it defaulted. In some cases a company can file to the court for some kind of relief from the debts, which then offers an opportunity to the debtor to become liquid again, and helps the creditor to regain the borrowed value to some extent. Since the financial market consists of a variety of companies with many sorts of interdependencies, one such action is bound to propagate from the two actors in the process deeper into the system. This process can trigger further defaults and can manifest itself as a cascade of significant size [14–16]. It is believed that such cascades can sometimes completely destroy financial system or the whole economy.

Financial contagion on networks is usually modeled using balance sheets of nodes, where different categories in the balance sheet insulate against financial distress. Explicit modelling of financial contagion via balance sheets appears in [5]. Kobayashi *et al.* in [17] illustrates the equivalence of the balance sheet approach with the threshold model of cascades presented in [18]. In [19] Acemoglu *et al.* explore network architecture contributing to or insulating against financial contagion between banks. On the other hand, very few papers exist that study transmission of financial shock between firms. Acemoglu *et.al.* in [20], as well as [21] and [22] aim to develop network theory of production which would meaningfully model links between firms. Others, such as [23] construct a business network from supply chain

data. The main fault of these approaches is that they do not distinguish well between shock transmitted from other nodes as opposed to field effects that affect node failure. In other words, random failures that are a result of an exogenous shock to a node may seem like a cascade if a connected node failed as well.

Our research was motivated by some of authors previous involvement in investigation of such effects in data of financial networks. In this case the problem was treated using randomized reference models [24] on a directed temporal network with the companies and their times of default on vertices, and their mutual debts on edges, pointed from borrower to lender [25]. The amount of debt that potentially caused the default of the lender (the default of the borrower happened before it) was counted on the original network, and then on the ensemble of networks with shuffled vertex times. The signal of internal dynamics of defaults was detected through a significant p-value of this amount of debt.

Randomized reference models were also used in temporal embedding [26], inference of structures in communication networks [27] and analysing collective behaviour in social networks [28].

Network motifs have a long tradition of being used as a tool for inference in complex networks [29]. They are small subgraphs that can be observed with different frequencies in the data. They were previously used to understand metabolic and other biological networks [29–31]. Furthermore, they were also used to understand the properties of ecological system through food webs [32], in economical setting to understand corporate governance [33, 34], and to understand organization of knowledge in Wikipedia [35]. Motif analysis was also efficiently extend to temporal networks [36].

Another line of research relevant for this work is inference of external and internal influence on propagation of information. Previous works were mainly embedded in social networks and question is the influence of peers in network dominant to outside influences or not [37–39]. The direction of this research is mostly related to estimation of parameters to proposed models of information spreading.

II. OBJECTIVES

Our aim was to extend the methodology for detection of default cascades, developed in the previous work[25], by making the structure of interactions more complex. In addition to single edges, we will introduce *causal motifs* with two and three edges and the largest component of causal edges as variables we use for the test statistics, but will omit any other data like weights in order to make the method usable as many situations as possible. This

methodology should in principle be applicable to any spreading phenomena (with two states) on any directed network. In this paper we will use jargon adapted for original economic application, but one can easily translate it to more general framework. Borrower is the vertex from which directed edge is originating, Lender is the vertex into which directed edge finishes and default is the change of the state of the vertex.

We assume that the data at hand are similar to data we collected i.e. that we know *at least* the timestamp of vertex default (change of state) with good enough resolution that times of defaults can be ordered. We also assume that we know the vertices to which borrower vertex was indebted. Therefore we have data of defaulted borrowers which defaulted at time t and a list of their lenders. We further assume that we do not know the exact mechanics of default or that we are missing some crucial information, for instance the assets and liabilities of each company or even the monetary value of credit between vertices. We could in principle include this data, but as stated before, our goal here is also to develop a very robust method which assumes smallest amount of information available and is therefore applicable in the broadest possible context.

Having only this data the question arises: Can we detect if default cascades are propagating through the credit network?

In the real world there is a myriad of scenarios resulting in defaults of companies. Sometimes it can be related mainly to exogenous events like for instance loss of market access, loss of access to finance, monetary shocks etc. In other cases the defaults in the system (network) are mostly endogenous and are related to inability of different actors (vertices) to fulfill their obligation to their lenders. This type of events is common in financial systems that are not well regulated and it is believed to be a significant contributor to largest systemic events even in the well regulated systems. We should be able to detect this endogenous events in time to act.

In order to validate our methodology in any of aforementioned cases, besides original data of company defaults, we create artificial data for detection of cascades using the developed methodology and determine which type of motifs is the most successful test statistic. For convenience all the programs used in this paper and company default data are available in our Git-Hub repository of supplementary information [40].

III. METHODOLOGY

Here we describe the rationale for our methodology. If there are no lenders that are also borrowers in the data, then there is no contact process present,

i.e. even if there would be a small chance that some debtor could cause the default of its lender in the future, in the present data we are not able to observe it. When there exist borrowers which are also lenders, we can assume two possible scenarios. In the first one, the default of that vertex is completely related to exogenous causes and the connection of the lender and its borrower is irrelevant for the default of the lender - perhaps the credit was too small to significantly influence the financial stability of the lender, or there exists an institution that will repay the borrower's obligations to the lender. In the second scenario the default of the borrower at time t_1 *causes* the default of at least one of its lenders. This lender is then present in the data as defaulted at the later time t_2 . One can observe that in the first scenario the default of the lender and borrower can happen in any order, while in the second the order is clear t_1 has to happen before t_2 .

Notice that the unknown default mechanisms for any of the cases *can not* change this very basic causal relationship. Whichever is the true mechanism that causes vertices in the data to default, *we expect* that the pattern of time stamps on the network in which defaults are driven by purely exogenous process will be very different from the time stamp pattern generated by the default process which has an endogenous component.

Based on this observation we will count the motifs [29] which have a purely causal structure in the data to see if their count can be explained by a solely exogenous process. This means that directed edge pointing from i to j will be associated with timestamps of defaults t_i and t_j of the vertices and we will call this edge *causal edge* if $t_i < t_j$. We will also define a *causal motif* as any motif in which *all* the edges are causal. Examples of such causal motifs are presented in Table I. Our assumption is that such causal motifs will be less common if the process is purely exogenous as compared with the mixed case in which both exogenous and endogenous dynamics exist. Therefore our null-hypothesis will be that the frequency of observed causal motifs is completely consistent with the purely exogenous default mechanism.

Similar type of ordered motifs were previously introduced in the case of food webs and were called *ordered motifs* [41], but in that case values describing ordering had different probability of being in or out, while in this case older defaults *have to* precede younger and therefore our motifs represent a special case of ordered motifs. Such strictly time ordered motifs we call *causal motifs*.

Another very recent related work defines *process motifs* [42] as building blocks of dynamical systems operating on network. In this case process motifs are a small graphs composed of *walks* on them. Authors then compute specific contributions of struc-

tural motifs from contributions of process motifs and use them as indicators of efficient mechanisms to increase some property of dynamical system.

Yet another usage of temporal motifs can be found in [43], in which authors use similar concept to ours to detect anomalies in time series on networks.

In previous works motifs are usually related to the number of vertices that comprise these motifs. Here causal motifs are ordered by the number of edges that comprise them. Since every contact process uses edges for propagation, this choice of convention is natural for stated aim of distinguishing patterns generated by endogenous process from patterns generated by exogenous process. All the causal motifs up to and including order 3 are depicted in table I.

We reiterate again that in purely exogenous defaults time does not play any role i.e. the default of the vertex can not cause the default of other vertex and therefore they could have defaulted in principle in any order with respect to information we have at hand. Therefore the purely exogenous process should not depend on the timestamps that are present in the data and in principle any vertex could have defaulted at any time compared to any other vertex. That means that we can permute the time stamps of defaults and we will create just as likely set of default events as in the original data.

Our methodology will therefore be based on the permutation of timestamps, creation of a new instance of data and counting the number of causal motifs of given kind. Then we will compare how often in the permuted data we can count the same or larger number of motifs. For that matter, a micro-canonical randomized reference model [24] will be created by shuffling the times on the defaulted vertices and keeping all the other network properties constrained. A distribution of motif counts will be obtained from the ensemble and compared to the count one obtains from the data or from simulation of stochastic cellular automata process.

While we use simulations to perturb timestamps in data it is instructive to first consider what frequency of the motifs would one expect if only exogenous process changes the state of vertices in the network. In that case probability of finding each individual causal motif \mathcal{CM} would be (i) proportional to probability $p(\mathcal{M})$ of finding the structural motif \mathcal{M} on which a causal motif could develop; (ii) probability $\mathcal{P}(T)$ that all the vertices of the given motif \mathcal{M} have changed their state (got infected, have defaulted) by the time T ; and (iii) the probability that the vertices in the motif \mathcal{M} have defaulted in such an order that all the edges of the motif have become causal.

The third probability can in principle be computed from pure combinatorics because only the mutual ordering of timestamps is of importance and not their frequency of occurrence or any other details of

Causal Motif	Probability	Causal Motif	Probability
	$p(\mathcal{M}) \frac{1}{2} \pi(T)^2$		$p(\mathcal{M}) \frac{1}{8} \pi(T)^4$
	$p(\mathcal{M}) \frac{1}{6} \pi(T)^3$		$p(\mathcal{M}) \frac{1}{8} \pi(T)^4$
	$p(\mathcal{M}) \frac{1}{3} \pi(T)^3$		$p(\mathcal{M}) \frac{1}{4} \pi(T)^4$
	$p(\mathcal{M}) \frac{1}{3} \pi(T)^3$		$p(\mathcal{M}) \frac{1}{4} \pi(T)^4$
	$p(\mathcal{M}) \frac{1}{24} \pi(T)^4$		$p(\mathcal{M}) \frac{5}{24} \pi(T)^4$
	$p(\mathcal{M}) \frac{1}{12} \pi(T)^4$		$p(\mathcal{M}) \frac{1}{6} \pi(T)^3$
	$p(\mathcal{M}) \frac{1}{12} \pi(T)^4$		

TABLE I: Table with all possible causal motifs up to order 3.

temporal process. So for example for the third motif in the leftmost column of table, all that is important is that t_1 is the earliest timestamp out of three timestamps and that randomly occurs 1/3 of the time.

In order to compute even higher order motifs than the one presented here we found that using integrals

over exogenous probability per unit time is simpler. Let us suppose that the exogenous probability per unit time of the state of change of the individual vertex is $\phi(t)$. Then we could write an equation to obtain 3 edge causal motif that looks like letter N in Table I as:

$$\begin{aligned}
 P(\mathcal{CM}) &= p(\mathcal{M}) \int_0^T \int_0^{t_3} \left(\int_0^{t_3} \phi(t_1) dt_1 \int_{t_2}^T \phi(t_4) dt_4 \right) \phi(t_2) \phi(t_3) dt_2 dt_3 \\
 &= p(\mathcal{M}) \int_0^T \int_0^{t_3} \pi(t_3) [\pi(T) - \pi(t_2)] \phi(t_2) dt_2 \phi(t_3) dt_3 \\
 &= p(\mathcal{M}) \frac{5}{24} \pi(T)^4,
 \end{aligned} \tag{1}$$

where we used $\pi(\tau) = \int_0^\tau \phi(t) dt$, and the relation between cumulative probability and probability density $\int \phi(t) dt \equiv \int d\pi(t)$.

As we see in the Table I, all the higher order motifs are becoming less and less probable to be found with respect to purely exogenous process and as a starting

point we will use the count for each motif order as the statistics to test if the data could be explained only through exogenous process. Therefore for each motif order we will use the count $\mathcal{N}(t)$ in time t as a testing variable that will be compared against the randomized reference model.

Alternatively we will separate the motifs within each order and compute Mahalanobis distance as a generalization of Z-score, to get more information. In Table I it is clear that the "train" motif of just sequence of causal edges is the least probable to be created by chance (exogenous process) compared to others of the same order. We expect that this difference within the motifs of given order will be more sensitive to the possible existence of endogenous process.

Therefore for each count of causal motifs we will create a vector $\mathbf{C}^{(i)}$ whose components represent the count of every type of motifs of order i found in the network. Dimension of this vector will be 1 for 1 edge motifs, 3 for two edge motifs and 9 for three edge motifs. After reshuffling of times in the network one can compute Mahalanobis distance $D^{(i)}$ of the causal motifs of order i given as:

$$D^{(i)} = \sqrt{(\mathbf{C}^{(i)} - \mu^{(i)})^T \Sigma_i^{-1} (\mathbf{C}^{(i)} - \mu^{(i)})}, \quad (2)$$

where $\mu^{(i)}$ is average motif vector obtained in time reshuffled networks, and Σ_i is a covariance matrix of the vector counts in reshuffled networks. In the case of diagonal covariance matrix Mahalanobis distance is the square root of the sum of squares of z-scores of each vector component (individual causal motif). This property guarantees that Mahalanobis distance is always greater or equal to each of individual z-scores, and it makes it more sensitive to detection of endogenous propagation. In order to better understand the value of this distance one can use unbiased estimator of p-value from Mahalanobis distance [44].

Lastly we will use the largest causally connected component as test statistics. The definition of this component is equivalent to the definition of the largest weakly connected component [45] in the network in which all edges except causal are deleted.

We validate the methodology on data created by simulating default processes on synthetic networks. Erdős-Rényi graphs are used as the underlying networks. We set the number of vertices N and the expected degrees $\langle k_{in} \rangle$ and $\langle k_{out} \rangle$ to generate an ensemble of N_{graph} directed networks. On each network a process of companies defaulting is determined by process parameters α and β , and simulated $N_{process}$ times.

The simulation is composed of two Poisson processes, used for sampling exogenous and endogenous default inter event times, with rates α and $\beta_i = x_i \beta$, respectively. The endogenous rate is defined as a value common to the entire network β , weighted by

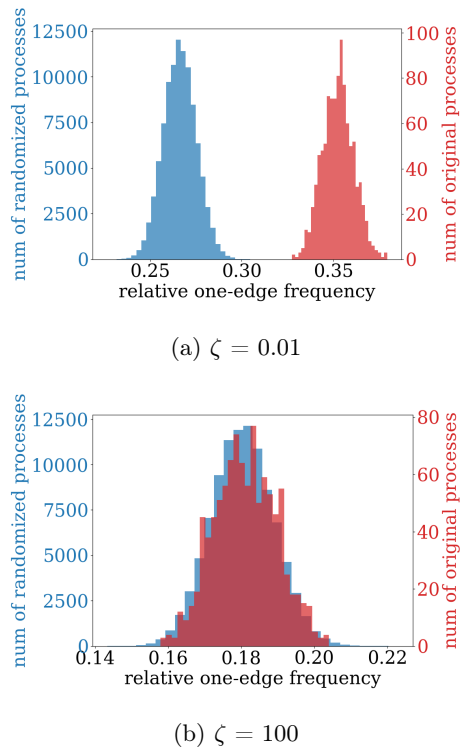


FIG. 1: Original(red) and shuffled (blue) one-edge statistic histograms on a 60% defaulted networks for different ζ

some inherent vertex property x_i . Event times are therefore drawn from the exponential distribution with CDF:

$$F(t; \lambda) = 1 - e^{-\lambda t}, \quad t \geq 0, \quad \lambda = \alpha, x_i \beta \quad (3)$$

The weight x_i will be set depending on the class of contact process used; SI type of process, as the simplest propagation process has $x_i = 1, \forall i$, while voter model weighs the rate of a vertex i as $x_i = 1/k_i^{in}$.

We define a chronologically ordered list of potential default times $\mathbf{t}^D = \{t_i^D\}$ and fill it with the set of α -event times. The process starts at the vertex i with the first time t_1 from the list. The time of the default is then recorded as a property of the vertex. β_j -inter event times, associated with the out-edges, are added to the time of the default; for a vertex j connected to the source vertex i with an edge $l = (i, j)$ the potential default time caused by the default of i is:

$$\begin{aligned} t_{j(SI)}^\beta &= t_i^\alpha + \Delta t_{(i,j)}^\beta, \quad \text{or} \\ t_{j(VM)}^{\beta/k_j^{in}} &= t_i^\alpha + k_j^{in} \Delta t_{(i,j)}^\beta \end{aligned} \quad (4)$$

depending whether we wish to simulate an SI or voter model (VM) type of endogenous component.

IV. ANALYTICAL EXPLANATION

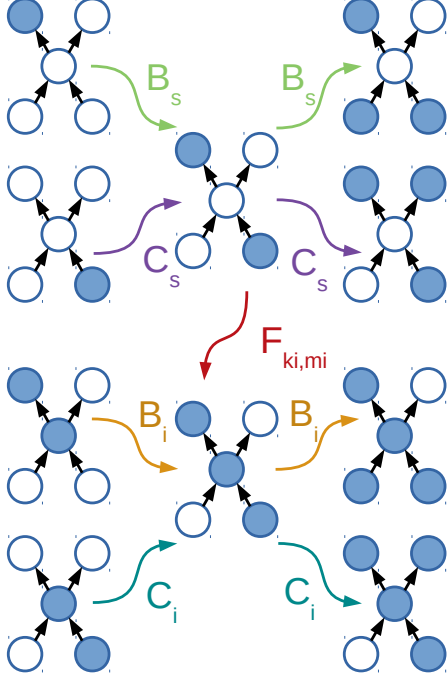


FIG. 2: This figure represents the AME states and probabilities of transition from one state to another. Central transition F_{k_i, m_i} , represents changing of the state of the central vertex that we are interested in, while B_s , C_s , B_i and C_i represent mean-field like transitions on neighboring vertices.

All t_i^β from this step are added to the chronologically ordered list t^D accordingly. Note that a single vertex can have several potential default times, however only the smallest one will be recorded as its real default time. After the list is updated, the vertex with the first time defaults next and the aforementioned potential default spreading is repeated. The process continues until all vertices are defaulted.

By changing the ratio $\zeta := \alpha/\beta$ we control the endogenous component of the simulated process. To gain better insight into the dynamics of defaults, we stop the process after every 5 % of the original network's vertices default and record the size of the largest component and the count of each motif.

After every pause, distributions of the count of motifs and the size of the largest component are obtained from the ensemble of time-shuffled networks.

Finally we obtain a distribution of each statistic for the original process on the network and the distribution of the statistic on the randomized reference model, for every percentage of the network that defaulted as is depicted in Fig. 1

To obtain an analytical expression for the macroscopic quantities of interest, we employ the Approximate Master Equations (AME) [46] and generalize them to directed networks with causal edges. Here we assume that the network is completely connected in a weak sense (some vertices can have only in or only out edges attached to them) and that it can have correlations on vertices i.e.

$$P(k_i, k_o) \neq P(k_i)P(k_o). \quad (5)$$

Although, we are focused on our immediate application to the network of defaults in the economy, we will use language of epidemic spreading to make reading of the paper easier and related to language of [46].

Therefore, let S_{k_i, k_o, m_i, m_o} (resp. $I_{k_i, k_o, m_i, m_o, z_i, z_o}$) be the set of vertices which are susceptible (resp. infected), have in-degree k_i , out-degree k_o and have m_i and m_o infected neighbors on their incoming (resp. outgoing) edges, which we can further subset to z_i and z_o causally infected vertices ($z_i = z_o = 0$ by definition for susceptible vertices). In economic terms susceptible vertices are those which are financially healthy, while infected are those with financial problems or which have defaulted. On these sets we define measures s_{k_i, k_o, m_i, m_o} and $i_{k_i, k_o, m_i, m_o, z_i, z_o}$ which represent the fraction of vertices that are susceptible or infected among the vertices that have their $\{k_i, k_o, m_i, m_o, z_i, z_o\}$ parameters.

Clearly,

$$1 = s_{k_i, k_o, m_i, m_o} + i_{k_i, k_o, m_i, m_o}, \quad (6)$$

$$i_{k_i, k_o, m_i, m_o}^z \equiv \sum_{z_i=0}^{k_i} \sum_{z_o=0}^{k_o} i_{k_i, k_o, m_i, m_o, z_i, z_o}, \quad (7)$$

$$i_{k_i, k_o, z_i, z_o}^m \equiv \sum_{m_i=0}^{k_i} \sum_{m_o=0}^{k_o} i_{k_i, k_o, m_i, m_o, z_i, z_o}. \quad (8)$$

Also the total fraction of infected (defaulted) vertices in the network, with in-degree k_i and out-degree k_o , is defined as

$$\begin{aligned} \rho_{k_i k_o}(t) &= \sum_{m_i=0}^{k_i} \sum_{m_o=0}^{k_o} i_{k_i, k_o, m_i, m_o}^z \\ &= 1 - \sum_{m_i=0}^{k_i} \sum_{m_o=0}^{k_o} s_{k_i, k_o, m_i, m_o}, \end{aligned} \quad (9)$$

Then the total number of infected vertices in a network containing N vertices is found by

$$\rho(t) = N \sum_{k_i, k_o} P(k_i, k_o) \rho_{k_i, k_o}(t). \quad (10)$$

Next, we examine how the sizes of the S_{k_i, k_o, m_i, m_o} and $I_{k_i, k_o, m_i, m_o, z_i, z_o}$ sets change in time. We write

the general expression for the fractions of susceptible and infected vertices:

$$\begin{aligned}
s_{k_i, k_o, m_i, m_o}(t + dt) &= s_{k_i, k_o, m_i, m_o}(t) - W(S_{k_i, k_o, m_i, m_o} \rightarrow I_{k_i, k_o, m_i, m_o, z_i=m_i, z_o=0}) s_{k_i, k_o, m_i, m_o} dt \\
&\quad + W(S_{k_i, k_o, m_i-1, m_o} \rightarrow S_{k_i, k_o, m_i, m_o}) s_{k_i, k_o, m_i-1, m_o} dt \\
&\quad + W(S_{k_i, k_o, m_i, m_o-1} \rightarrow S_{k_i, k_o, m_i, m_o}) s_{k_i, k_o, m_i, m_o-1} dt \\
&\quad - W(S_{k_i, k_o, m_i, m_o} \rightarrow S_{k_i, k_o, m_i+1, m_o}) s_{k_i, k_o, m_i, m_o} dt \\
&\quad - W(S_{k_i, k_o, m_i, m_o} \rightarrow S_{k_i, k_o, m_i, m_o+1}) s_{k_i, k_o, m_i, m_o} dt \\
i_{k_i, k_o, m_i, m_o, z_i, z_o}(t + dt) &= i_{k_i, k_o, m_i, m_o, z_i, z_o}(t) + W(S_{k_i, k_o, m_i, m_o} \rightarrow I_{k_i, k_o, m_i, m_o, z_i=m_i, z_o=0}) s_{k_i, k_o, m_i, m_o} dt \\
&\quad + W(I_{k_i, k_o, m_i-1, m_o, z_i, z_o} \rightarrow I_{k_i, k_o, m_i, m_o, z_i, z_o}) i_{k_i, k_o, m_i-1, m_o, z_i, z_o} dt \\
&\quad + W(I_{k_i, k_o, m_i, m_o-1, z_i, z_o-1} \rightarrow I_{k_i, k_o, m_i, m_o, z_i, z_o}) i_{k_i, k_o, m_i, m_o-1, z_i, z_o-1} dt \\
&\quad - W(I_{k_i, k_o, m_i, m_o, z_i, z_o} \rightarrow I_{k_i, k_o, m_i+1, m_o, z_i, z_o}) i_{k_i, k_o, m_i, m_o, z_i, z_o} dt \\
&\quad - W(I_{k_i, k_o, m_i, m_o, z_i, z_o} \rightarrow I_{k_i, k_o, m_i, m_o+1, z_i, z_o+1}) i_{k_i, k_o, m_i, m_o, z_i, z_o} dt
\end{aligned} \tag{11}$$

and represent it graphically in Fig. 2.

Equation (11) accounts for the transitions which are linear in dt , as all the other transitions vanish in the limit of $dt \rightarrow 0$. The fundamental transition probability describes the transition from the set S_{k_i, k_o, m_i, m_o} to $I_{k_i, k_o, m_i, m_o, z_i, z_o}$ and is denoted $W(S_{k_i, k_o, m_i, m_o} \rightarrow I_{k_i, k_o, m_i, m_o, z_i=m_i, z_o=0})$. The transition probability consists of an exogenous and an endogenous component, as described in the Methodology section. We describe the exogenous process of vertex defaults with a rate of default α , and for the endogenous process of vertex defaults we use either the SI process or the voter model, determined by a rate of default infection β , as defined in:

$$\begin{aligned}
W(S_{k_i, k_o, m_i, m_o} \rightarrow I_{k_i, k_o, m_i, m_o, z_i=m_i, z_o=0}) &= F_{k_i, m_i} \\
F_{k_i, m_i}^{SI} &= \alpha + m_i \beta \\
F_{k_i, m_i}^{VM} &= \alpha + \frac{m_i}{k_i} \beta
\end{aligned} \tag{12}$$

The transition probability of the central vertex is described exactly by Eq. (12). As we have limited our sets to central vertices and their first neigh-

hours, to obtain the probabilities of the neighbours' transitions we need to approximate the effect the rest of the network has on them as mean field, using AME. Therefore, rates concerning defaults of neighbouring vertices in Equation 11 are factored into the mean field change rate of edge type and the number of susceptible neighbours of the central vertex. In Fig. 2, these rates are described with B_s , C_s , B_i and C_i . We will use the following abbreviations: $k_i, k_o, m_i, m_o \equiv \vec{K}_s$, $k_i, k_o, m_i, m_o, z_i, z_o \equiv \vec{K}_i$, $k_i, k_o, m_i+1, m_o, z_i, z_o \equiv \vec{K}_i + \vec{e}_{m_i}$. For the first equation in 11 we have:

$$\begin{aligned}
W(S_{\vec{K}_s} \rightarrow S_{\vec{K}_s + \vec{e}_{m_i}}) &= B_s(k_i - m_i), \\
W(S_{\vec{K}_s - \vec{e}_{m_i}} \rightarrow S_{\vec{K}_s}) &= B_s(k_i - m_i + 1), \\
W(S_{\vec{K}_s} \rightarrow S_{\vec{K}_s + \vec{e}_{m_o}}) &= C_s(k_o - m_o), \\
W(S_{\vec{K}_s - \vec{e}_{m_o}} \rightarrow S_{\vec{K}_s}) &= C_s(k_o - m_o + 1)
\end{aligned} \tag{13}$$

The term B_s represents the rate of change of edges directed from a susceptible vertex into a susceptible vertex ($S \rightarrow S$) to edges directed from an infected vertex into a susceptible vertex ($I \rightarrow S$).

$$B_s dt = \frac{\sum_{k_i, k_o} P(k_i, k_o) \sum_{m_i}^{k_i} \sum_{m_o}^{k_o} (k_o - m_o) F_{k_i, m_i} s_{\vec{K}_s} dt}{\sum_{k_i, k_o} P(k_i, k_o) \sum_{m_i}^{k_i} \sum_{m_o}^{k_o} (k_o - m_o) s_{\vec{K}_s}}. \tag{14}$$

The denominator counts the number of $S \rightarrow S$ edges, while the numerator counts how many of

them change to $I \rightarrow S$ in a time interval dt . C_s is defined for the transition from $S \rightarrow S$ to $S \rightarrow I$,

and computed similarly.

$$C_s dt = \frac{\sum_{k_i, k_o} P(k_i, k_o) \sum_{m_i}^{k_i} \sum_{m_o}^{k_o} (k_i - m_i) F_{k_i, m_i} s_{\vec{K}_s} dt}{\sum_{k_i, k_o} P(k_i, k_o) \sum_{m_i}^{k_i} \sum_{m_o}^{k_o} (k_i - m_i) s_{\vec{K}_s}}. \quad (15)$$

For the second equation in (11), rates of neighbour infections, B_i and C_i , are defined analogously.

$$\begin{aligned} W(I_{\vec{K}_i} \rightarrow I_{\vec{K}_i + \vec{e}_{m_i}}) &= B_i(k_i - m_i), \\ W(I_{\vec{K}_i - \vec{e}_{m_i}} \rightarrow I_{\vec{K}_i}) &= B_i(k_i - m_i + 1), \\ W(I_{\vec{K}_i} \rightarrow I_{\vec{K}_i + \vec{e}_{m_o} + \vec{e}_{z_o}}) &= C_i(k_o - m_o), \\ W(I_{\vec{K}_i - \vec{e}_{m_o} - \vec{e}_{z_o}} \rightarrow I_{\vec{K}_i}) &= C_i(k_o - m_o + 1) \end{aligned} \quad (16)$$

After inserting the calculated rates into (11), dividing by dt and taking the limit $dt \rightarrow 0$, we get the differential equation for the evolution of the fraction of susceptible vertices:

$$\begin{aligned} \frac{d}{dt} s_{\vec{K}_s} &= B_s \left((k_i - m_i + 1) s_{\vec{K}_s - \vec{e}_{m_i}} - (k_i - m_i) s_{\vec{K}_s} \right) \\ &+ C_s \left((k_o - m_o + 1) s_{\vec{K}_s - \vec{e}_{m_o}} - (k_o - m_o) s_{\vec{K}_s} \right) \\ &- F_{k, m} s_{\vec{K}_s}, \end{aligned} \quad (17)$$

and of the fraction of infected vertices:

$$\begin{aligned} \frac{d}{dt} i_{\vec{K}_i} &= B_i \left((k_i - m_i + 1) i_{\vec{K}_i - \vec{e}_{m_i}} - (k_i - m_i) i_{\vec{K}_i} \right) \\ &+ C_i \left((k_o - m_o + 1) i_{\vec{K}_i - \vec{e}_{m_o} - \vec{e}_{z_o}} - (k_o - m_o) i_{\vec{K}_i} \right) \\ &+ F_{k, m} s_{\vec{K}_s, z_i=m_i, z_o=0}, \end{aligned} \quad (18)$$

The solutions $s_{\vec{K}_s}$ and $i_{\vec{K}_i}$ of the Eq. 17 and 18 are obtained numerically. Using $i_{\vec{K}_i}$, we can easily calculate the temporal evolution of the fraction of causal motifs with one and two edges, for the central vertex with k_i and k_o - $c_{k_i, k_o}^{(1)}(t)$ and $c_{k_i, k_o}^{(2)}(t)$, respectively.

$$\begin{aligned} c_{k_i, k_o}^{(1)}(t) &= \sum_{z_i=0}^{k_i} \sum_{z_o=0}^{k_o} z_o i_{k_i, k_o, z_i, z_o}^m(t) \\ c_{k_i, k_o}^{(2)}(t) &= \sum_{z_i=0}^{k_i} \sum_{z_o=0}^{k_o} \left(\binom{z_i}{2} + z_i z_o + \binom{z_o}{2} \right) \\ &\times i_{k_i, k_o, z_i, z_o}^m(t) \end{aligned} \quad (19)$$

The temporal evolution of the fraction of causal motifs with one and two edges, for the central vertex with k_i and k_o , when the time ordering of the

defaulted vertices is randomly distributed is denoted as $\tilde{c}_{k_i, k_o}^{(1)}(t)$ and $\tilde{c}_{k_i, k_o}^{(2)}(t)$ and equals :

$$\begin{aligned} \tilde{c}_{k_i, k_o}^{(1)}(t) &= \frac{1}{2} \sum_{m_i=0}^{k_i} \sum_{m_o=0}^{k_o} m_o i_{k_i, k_o, m_i, m_o}^z(t) \\ \tilde{c}_{k_i, k_o}^{(2)}(t) &= \sum_{m_i=0}^{k_i} \sum_{m_o=0}^{k_o} \left(\frac{1}{3} \binom{m_i}{2} + \frac{1}{6} m_i m_o + \frac{1}{3} \binom{m_o}{2} \right) \\ &\times i_{k_i, k_o, m_i, m_o}^z(t) \end{aligned} \quad (20)$$

If we want to calculate the mean value and the variance of causal motifs we only need to specify the distribution $P(k_i, k_o)$. The first two central moments for one and two edges are:

$$E[C^{(1,2)}] = N \sum_{k_i, k_o} P(k_i, k_o) c_{k_i, k_o}^{(1,2)}(t) \quad (21)$$

$$\begin{aligned} V[C^{(1,2)}] &= N \sum_{k_i, k_o} P(k_i, k_o) (c_{k_i, k_o}^{(1,2)}(t) - \\ &- \frac{1}{N} E[C^{(1,2)}(t)])^2 \end{aligned} \quad (22)$$

$$E[\tilde{C}^{(1,2)}(t)] = N \sum_{k_i, k_o} P(k_i, k_o) \tilde{c}_{k_i, k_o}^{(1,2)}(t) \quad (23)$$

$$\begin{aligned} V[\tilde{C}^{(1,2)}(t)] &= N \sum_{k_i, k_o} P(k_i, k_o) (\tilde{c}_{k_i, k_o}^{(1,2)}(t) - \\ &- \frac{1}{N} E[\tilde{C}^{(1,2)}(t)])^2 \end{aligned} \quad (24)$$

While expectations of motifs are correct in the above equations, the variance is just the *lower bound*. One can use the approach developed in [47] to obtain the correct variances but only for the purely exogenous case. In that case expected square of the number of one edge causal motifs on Erdős-Rényi

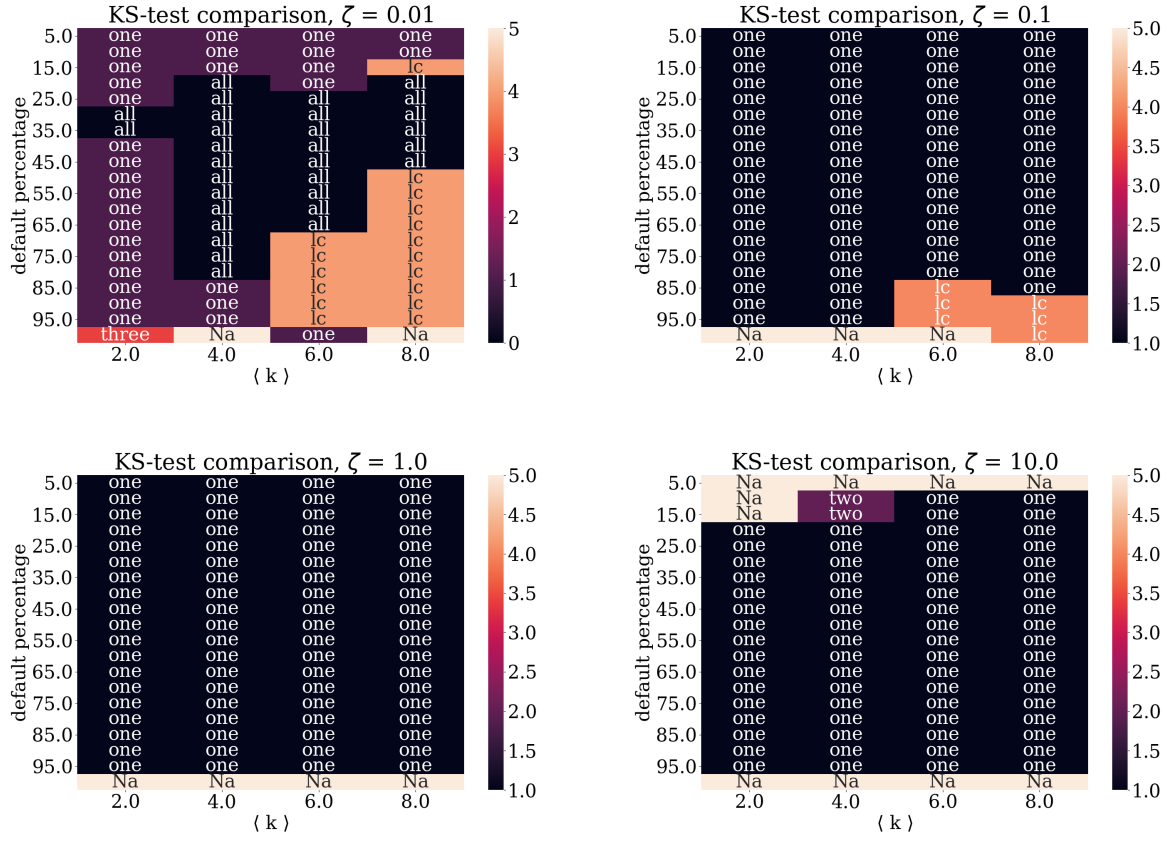


FIG. 3: Comparison of KS-test of the results for an SI process on a network of $N = 1000$ vertices. The best statistically significant statistic for a given percentage, ζ and $\langle k \rangle$ is stated as "lc" for largest component, "one" for one-edge, "two" for two-edge, etc. "Na" values mark the parameter space area where for all the test statistics the KS-result is statistically insignificant ($p > 0.1$), while "all" signifies that all the investigated motifs were able to easily distinguish the cases without statistical difference in performance.

network can be computed as:

$$\begin{aligned}
 E[C^{(1)}]^2 &= E\left[\sum_{a=k_i, k_o} \sum_{b=q_i, q_o} Y_a(C^{(1)}|t) Y_b(C^{(1)}|t)\right] \\
 &= \sum_{a=k_i, k_o} \sum_{b=q_i, q_o} E[Y_a(C^{(1)}|t) Y_b(C^{(1)}|t)] \\
 &= N(N-1)(N-2)(N-3)\left(p\frac{1}{2}\pi(t)^2\right)^2 + \\
 &\quad + N\binom{N-1}{2}p^2\frac{1}{3}\pi(t)^3 + \\
 &\quad + N(N-1)\left(p\frac{1}{2}\pi(t)\right)^2, \tag{25}
 \end{aligned}$$

where $Y_\alpha(C^{(1)}|t)$ similar to [47] represents indicator random variable of finding the causal motif of order one (causal edge) between two random vertices. Clearly the random indicator variable is connected to probabilities of occurrence of one and two edge causal motifs computed in Table I, p is just the probability of edge existing in the directed version of Erdős-Rényi graph.

With similar equations one can compute all the variances of purely exogenous process.

V. RESULTS

The final form of results, after generating N_{graph} different graphs, simulating $N_{process}$ processes on every graph, and creating $N_{shuffle}$ randomized reference models for each process, is a figure with two histograms (Fig. 1). One is the distribution of a statistic recorded on the original process, and the other the distribution of the statistic on the networks that result from time-shuffling. To quantify the difference between the distributions we use the two-sample Kolmogorov-Smirnov test. For a more precise comparison between one instance of a process and its null distribution we employ the z-score. Finally, to distinguish between the contributions of individual motifs within a class of motifs we use the Mahalanobis distance, which is a generalization of

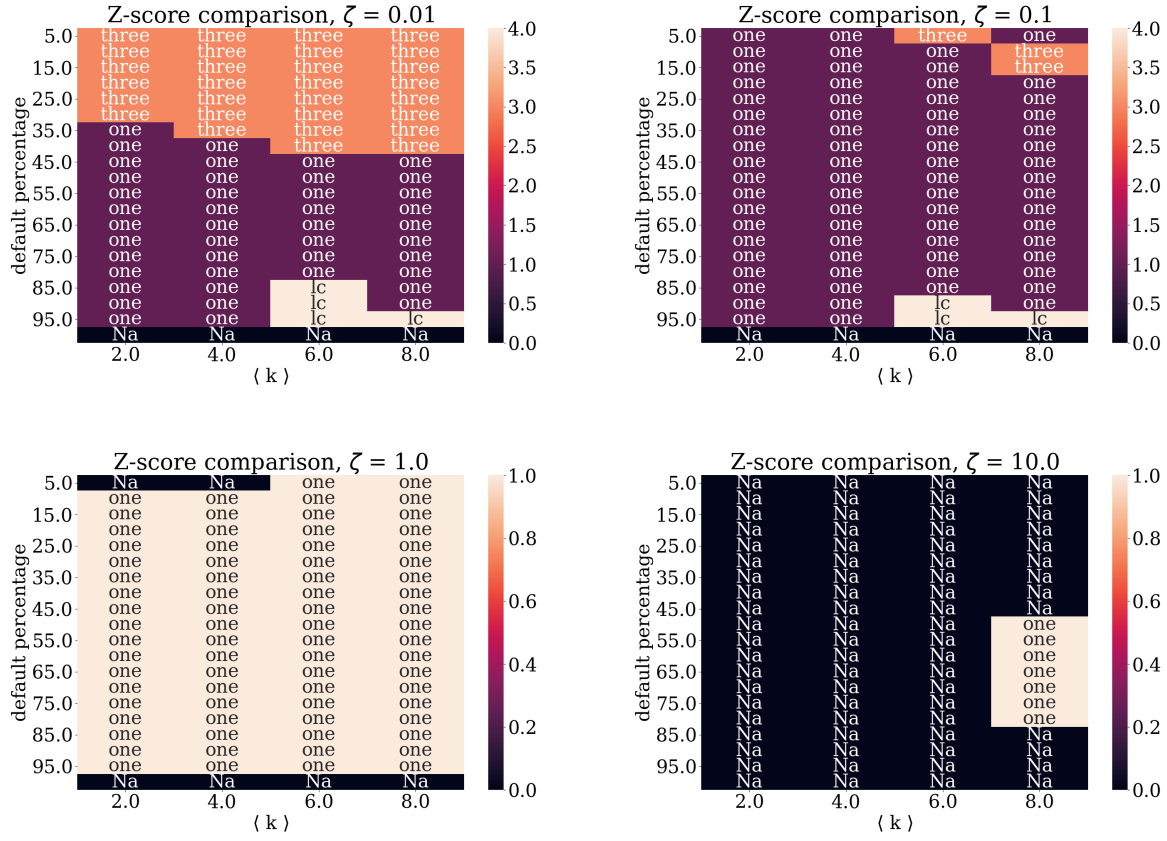


FIG. 4: Comparison of z-scores of the results for an SI process on a network of $N = 1000$ vertices. The best statistically significant statistic for a given percentage, ζ and $\langle k \rangle$ is stated as "lc" for largest component, "one" for one-edge, "two" for two-edge, etc. A z-score greater than 1 is considered to be statistically significant, otherwise an "Na" value is put in the table.

the z-score.

We also present the temporal evolution of simulated and calculated statistics and their variances in parallel. In the last section we will show the results of applying the methodology to the real data of Croatian companies' defaults.

A. SI model

In the first model of contagion we simulated we used a variant of an SI model as the endogenous component. Results are interpreted using the two sample Kolmogorov-Smirnov test (Fig. 3), a z-score (Fig. 4) and Mahalanobis distance. Temporal evolution of the statistics is shown for $\zeta = 0.1$ and $\langle k \rangle = 4$ in Fig. 6. More figures of temporal evolution are available in the supplementary information [40].

We first consider the distribution of simulated processes and compare it to the respective randomized distributions, using KS-test. From Fig. 3 we can see that the simplest causal motif - one-edge, pre-

vails for all simulated ζ parameters if the network degree $\langle k \rangle$ is 4 or less. However, for a greater degree ($\langle k \rangle = 6, 8$), causal largest component proves to be the best statistic. Causal motifs with two and three edges fail here because even though they separate first moments of the two distributions better, they also introduce a larger second moment.

Next, to provide a more detailed result, we make a comparison between each simulated process and its own randomized distribution, and quantify that with z-score. In Fig. 4 we see a similar prevalence of one-edge causal motif for networks with the mean degree $\langle k \rangle = 4$ or less, and the prevalence of the largest component for greater degrees and high percentages of network default. Nevertheless, for highly endogenous processes ($\zeta = 0.01$), the greatest causal motif, three-edge, is superior when below 50% of the network is defaulted, and that is more pronounced as the mean degree of the network grows. For $\zeta = 10.0$, one-edge statistic makes statistically significant ($z\text{-score} \geq 1$) separation only for $\langle k \rangle = 8$ in the middle part of the default process.

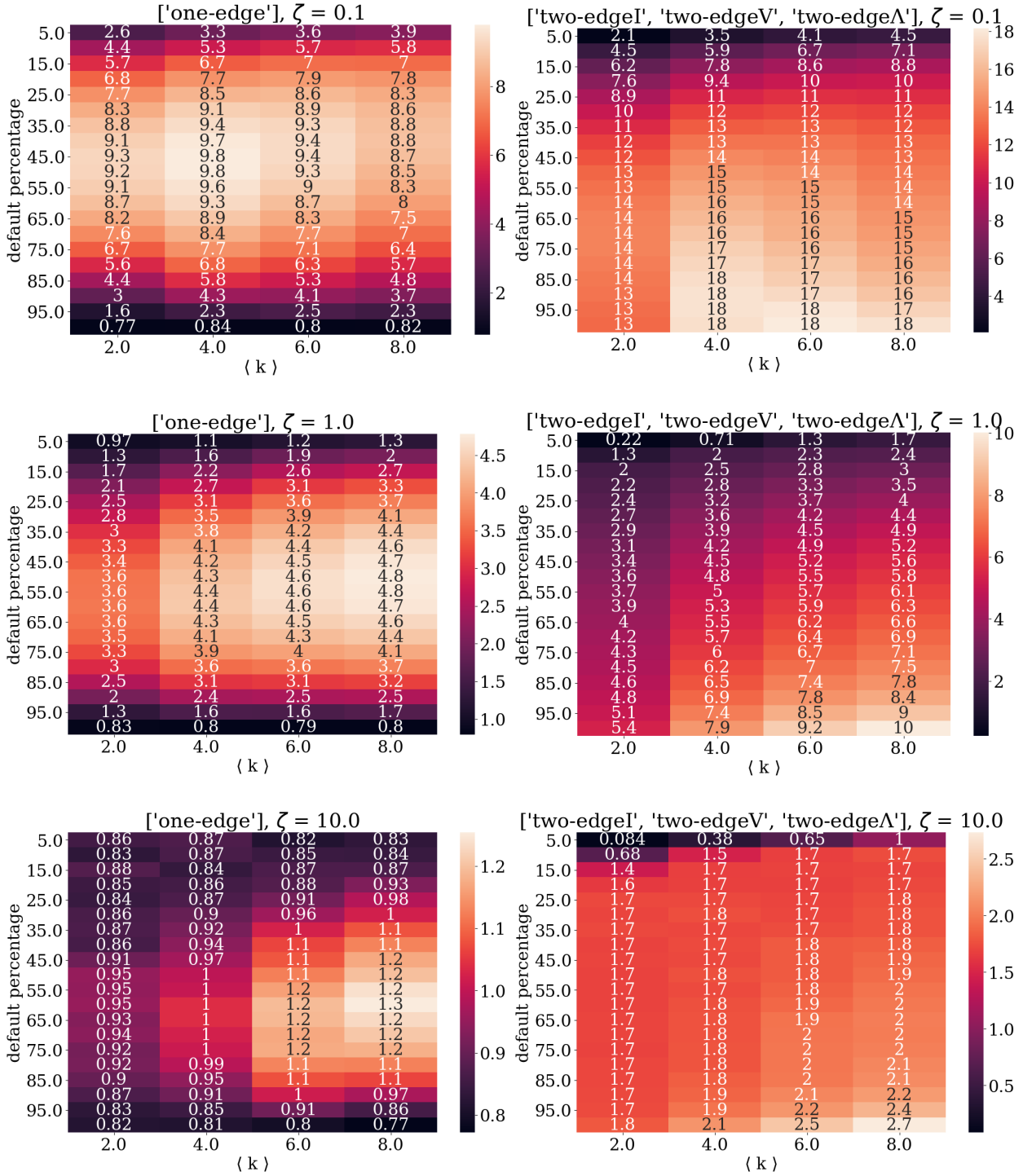


FIG. 5: Mahalanobis distances of the results for an SI process on a network of $N = 1000$ vertices. Results for one-edge and two-edge test statistics are given. The comparison of the statistics is given in the supplementary information [40]

In Fig. 6 we can see that the causal motif test statistics on both the original and randomized networks converge on average with time to a constant fraction of the total number of possible motifs. For

one-edge motifs that fraction is $1/2$ and for two-edge motifs $1/4$ of their total number. On randomized networks, where time ordering of the process is completely destroyed, that kind of convergence is

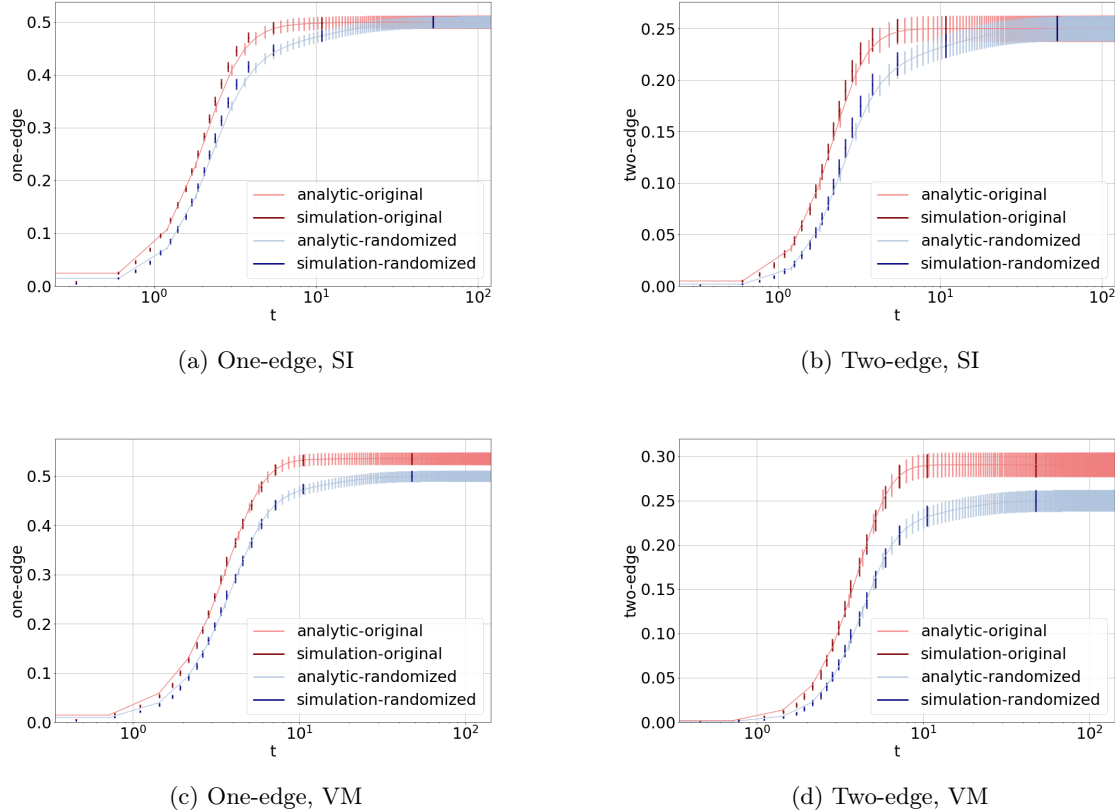


FIG. 6: One-edge and two-edge statistics for $\zeta = 0.1$ SI and VM process on an Erdős-Rényi graph with $N = 1000$, $\langle k \rangle = 4$. x-axis shows the time, while y-axis represents the relative frequency of a test statistic

expected.

Nevertheless, even with a strong endogenous driving, average numbers of causal motifs formed by an SI process converge in time to the same limits. If we observe a completely endogenous process of defaults until the default of all vertices on the Erdős-Rényi network, we can calculate the final number of causal one-edge motifs by summing the expected number of causal one-edge motifs in each step. The probability that one of the $\langle k_{out} \rangle$ outgoing edges reaches a susceptible vertex equals to the fraction of susceptible vertices $1 - t/N$, since the Erdős-Rényi network is homogeneous and the SI process treats all out-neighbours as equal. We see then that the number of causal one edges is:

$$C^{(1)} = \langle k_{out} \rangle \sum_{t=1}^N \frac{N-t}{N} = \frac{\langle k_{out} \rangle}{N} \frac{N^2 - N}{2} \approx \frac{N\langle k \rangle}{4} = \frac{L}{2} \quad (26)$$

Furthermore, we used Mahalanobis distance to compute contributions of individual submotifs to this case and showed it in Fig. 5. The square of the

Mahalanobis distance follows a chi-squared distribution, with the dimension of the data being equal to the degrees of freedom. Thus, the Mahalanobis distance is in general greater or equal than the z-score of a given motif, and it increases with the number of submotifs. In order to compare the results for statistics with different degrees of freedom, we employed the method from [48], which suggests dividing the chi-square statistic by the number of the degrees of freedom. From the results given in the supplementary information [40], we see that one-edge statistic is more useful at lower percentages of default, while two-edge statistic gives better distinguishing at higher percentages. As is seen the other tests, Mahalanobis distance obtains reliable distinguishing up to $\zeta = 1.0$.

B. Voter model

In the previous subsection we concluded that the properties of the Erdős-Rényi network and SI process cause causal motif test statistics from both original and randomized process to converge to the same limit. Therefore in addition to the SI variant of the

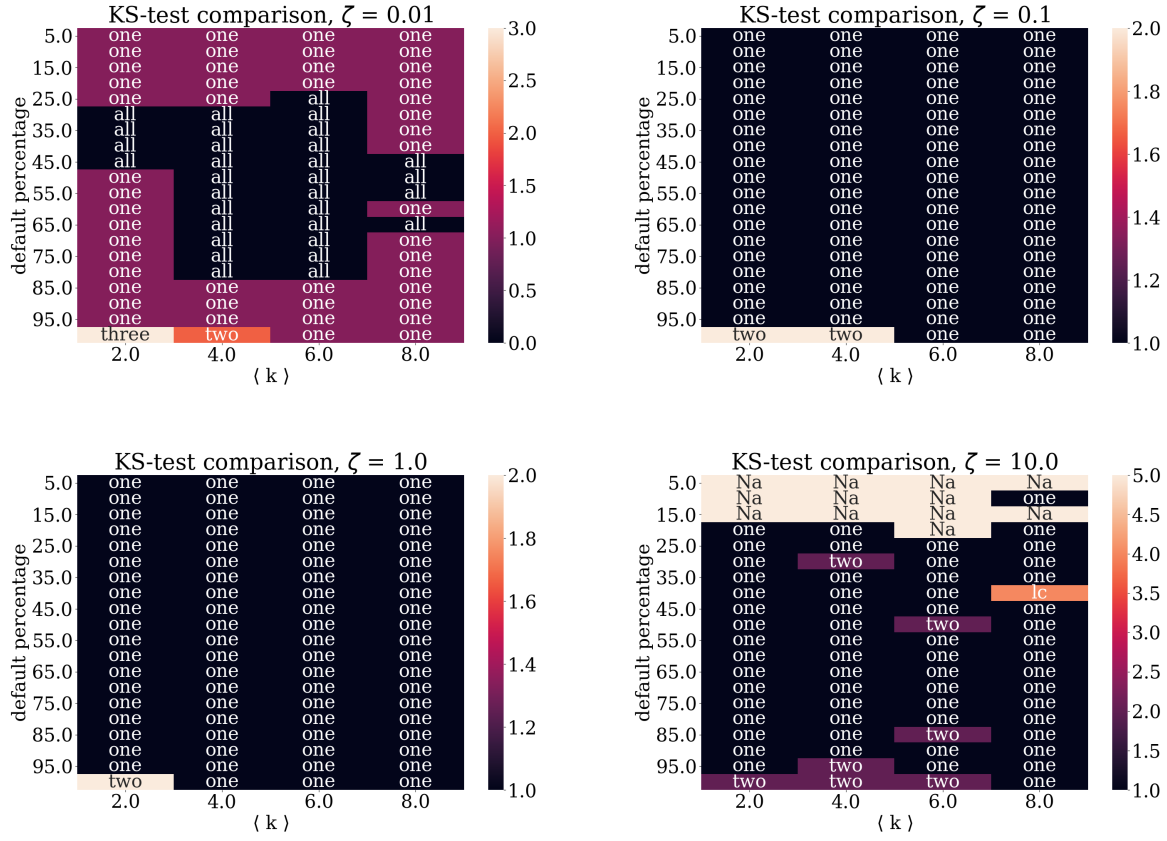


FIG. 7: Comparison of KS-test of the results for a voter model process on a network of $N = 1000$ vertices.

The best statistically significant statistic for a given percentage, ζ and $\langle k \rangle$ is stated as "lc" for largest component, "one" for one-edge, "two" for two-edge, etc. "Na" values mark the parameter space area where for all the test statistics the KS-result is statistically insignificant ($p > 0.1$), while "all" signifies that all the investigated motifs were able to easily distinguish the cases without statistical difference in performance.

endogenous component of the process, we consider the voter model variant, which introduces scaling the number of incoming defaulted vertices with the number of all incoming vertices per vertex.

It adds inhomogeneity in the defaulting process which allows the test statistic for the original process to have a different limit than for the random process, making the two more distinguishable, as it can be seen from Fig. 6c and 6d, where the temporal evolution of statistics is depicted.

KS-test results in Fig. 7 equivocally state that causal one-edge motif outperforms other test statistics in the case of endogenous voter model process. Since the causal motif distributions do not converge to the same limit, as in the case of SI process, one-edge dominates for all the simulated mean degrees $\langle k \rangle$.

Z-score results in Fig. 9 show a similar picture as for the SI endogenous component, with the three-edge causal motif being the best for very endogenous processes ($\zeta = 0.01$) up to 50% of network default,

and one-edge causal motif outperforming for all the other parameters. For $\zeta = 10.0$ none of the test statistics show a significant distinction.

We conclude that three-edge test statistic proves most robust at lower percentages of default for highly endogenous processes, while for all the other processes one-edge is the most successful test statistic.

The reason for this is that the variance of the higher order motifs grows faster than the separation between the centers of the distributions. Therefore, we employ the Mahalanobis distance (Fig. 8) on one- and two-edge motifs to make use of the sub-motif structure of the two-edge motif. The comparison between the different statistics is possible after squaring the results and dividing them by the number of the degrees of freedom, as the Mahalanobis distance is chi-square distributed with the dimensions of data as degrees of freedom. The results of the comparison are shown in the supplementary information [40], and we see that for $\zeta = 0.01, 0.1, 1.0$

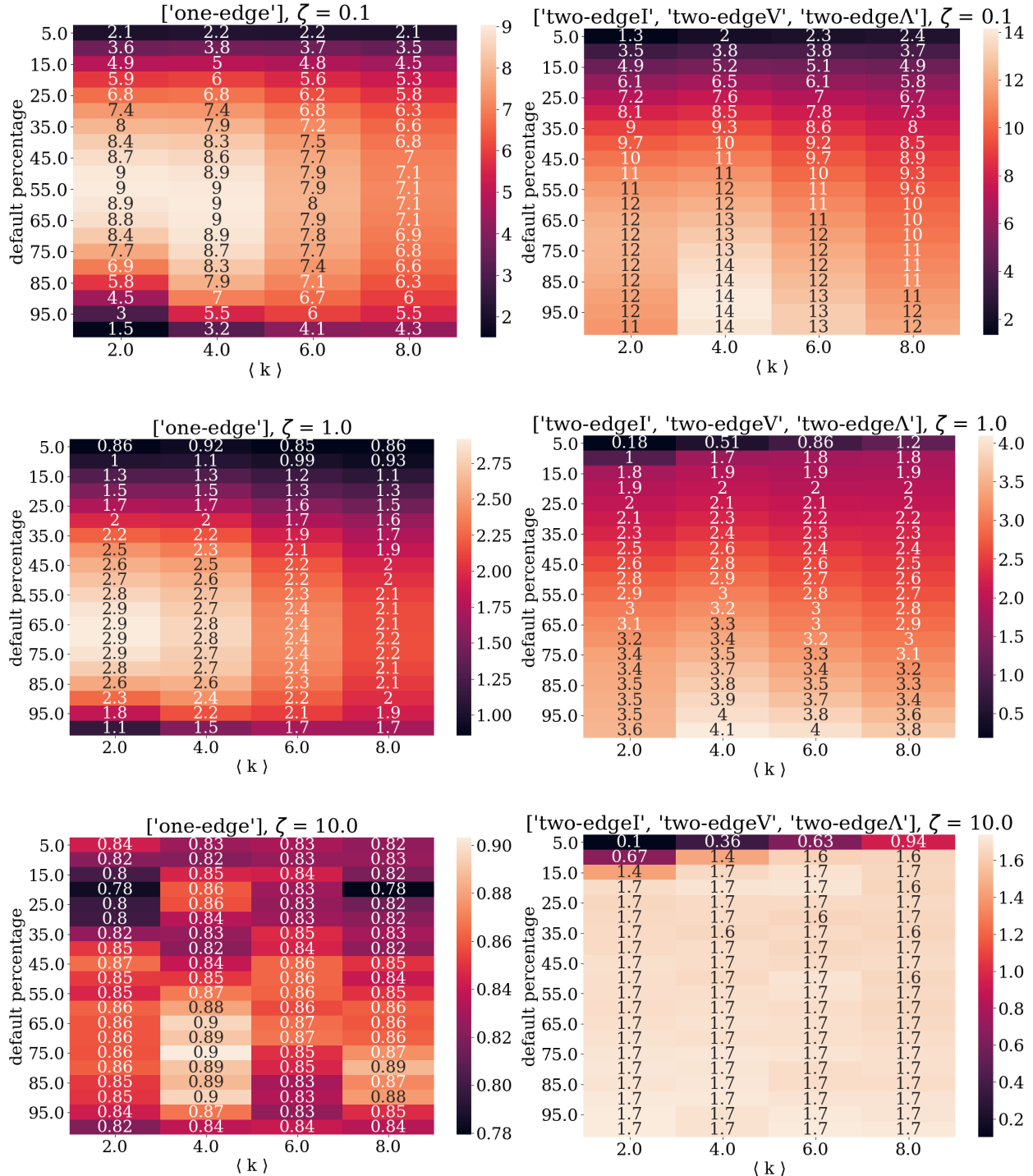


FIG. 8: Mahalanobis distances of the results for a voter model process on a network of $N = 1000$ vertices. Results for one-edge and two-edge test statistics are given. The comparison of the statistics is given in the supplementary information [40]

one-edge statistic is better at lower percentages of default, while two-edge statistic takes over for higher percentages. Other values of ζ do not show significant results.

C. Croatian Defaults

The data is collected from Croatian Financial Agency website which publicly discloses all doc-

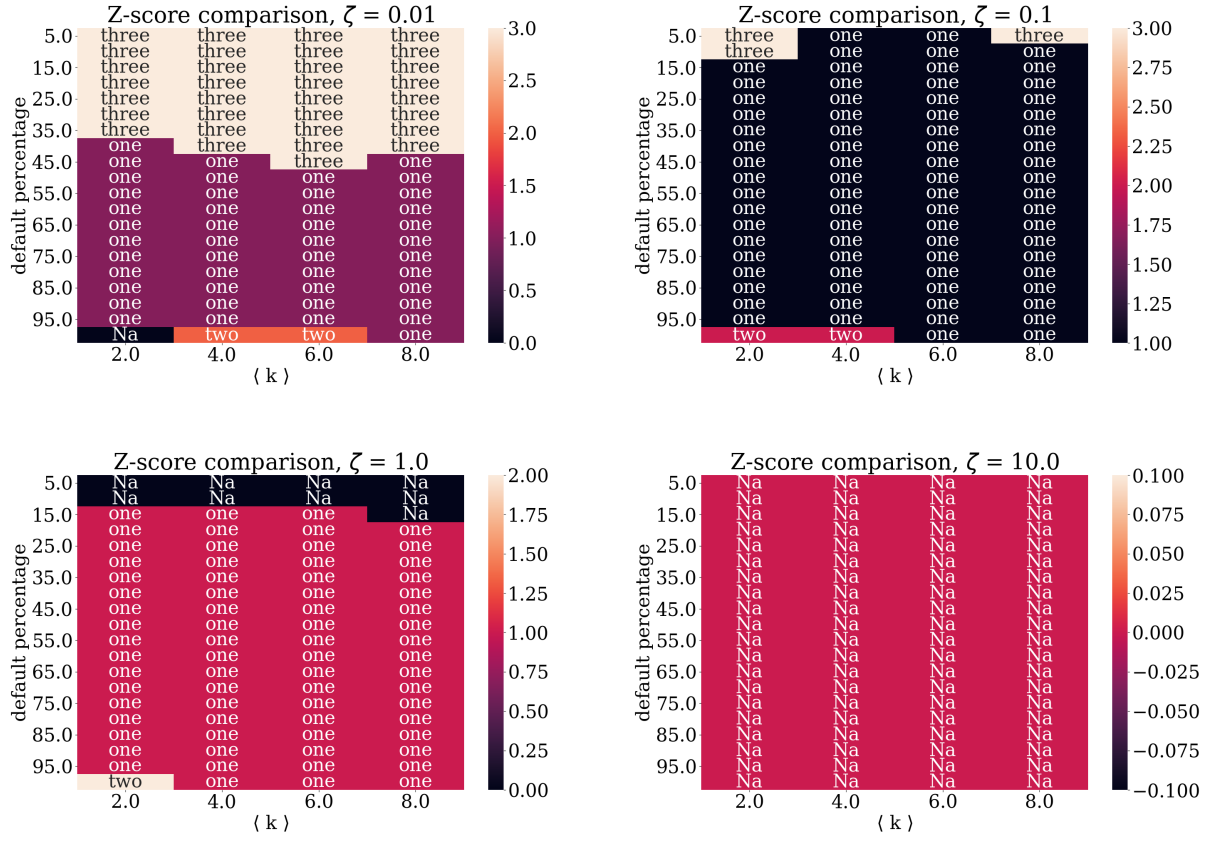


FIG. 9: Comparison of z-scores of the results for a voter model process on a network of $N = 1000$ vertices. The best statistically significant statistic for a given percentage, ζ and $\langle k \rangle$ is stated as "lc" for largest component, "one" for one-edge, "two" for two-edge, etc. A z-score greater than 1 is considered to be statistically significant, otherwise an "Na" value is put in the table.

ments related to Chapter 11 type bankruptcies which involved debt renegotiation and restructuring. A new law was passed at the end of 2012 which defined criteria companies had to meet in order to file for this type of bankruptcy: they failed to attain liquidity over the course of 60 days and at most 21 days passed since they became insolvent. The companies are obliged by law to list an extensive list of its creditors on the day they file for the procedure. However, the format of public data required extensive data mining and a big effort in cleaning these data to produce inputs which could be used in network formation.

The orderly data consists of a list of debtors, an exhaustive list of their creditors, the starting time and the length of the pre-bankruptcy settlement and the amount of debt per creditor. The data spans from December 19th 2012 to February 26th 2014, and contains 25469 vertices and 52507 edges, where debtors are exclusively firms and creditors range from banks, private and public firms, government and individuals. Total amount of reported debt was

5.97 billion euros, which corresponded to 13.6 percent of Croatia's GDP in 2014. The choice of specific time frame for dataset was intentional; in order to observe cascades, data collection began when the largest and most interconnected debtors filed for the procedure soon after the law was introduced at the end of 2012, following the initial illiquidity buildup, while number and size of firms significantly decreased in the next two years. Additionally, we only include recession years to avoid business cycle effects of economic recovery which may endogenously affect probabilities of defaults. i.e. may exert a different field effect on our network.

As we are trying to detect default cascades, we filter only the firms that can both have their own default caused endogenously, and spread the default into the network, that is, they have to be both debtors and creditors. Under that condition we are left with 549 firms, forming a network with 1198 edges (debts), a mean degree of 4.36 (mean out and in degree are 2.18), and maximal degree 60. Our method is then applied to the temporal network and

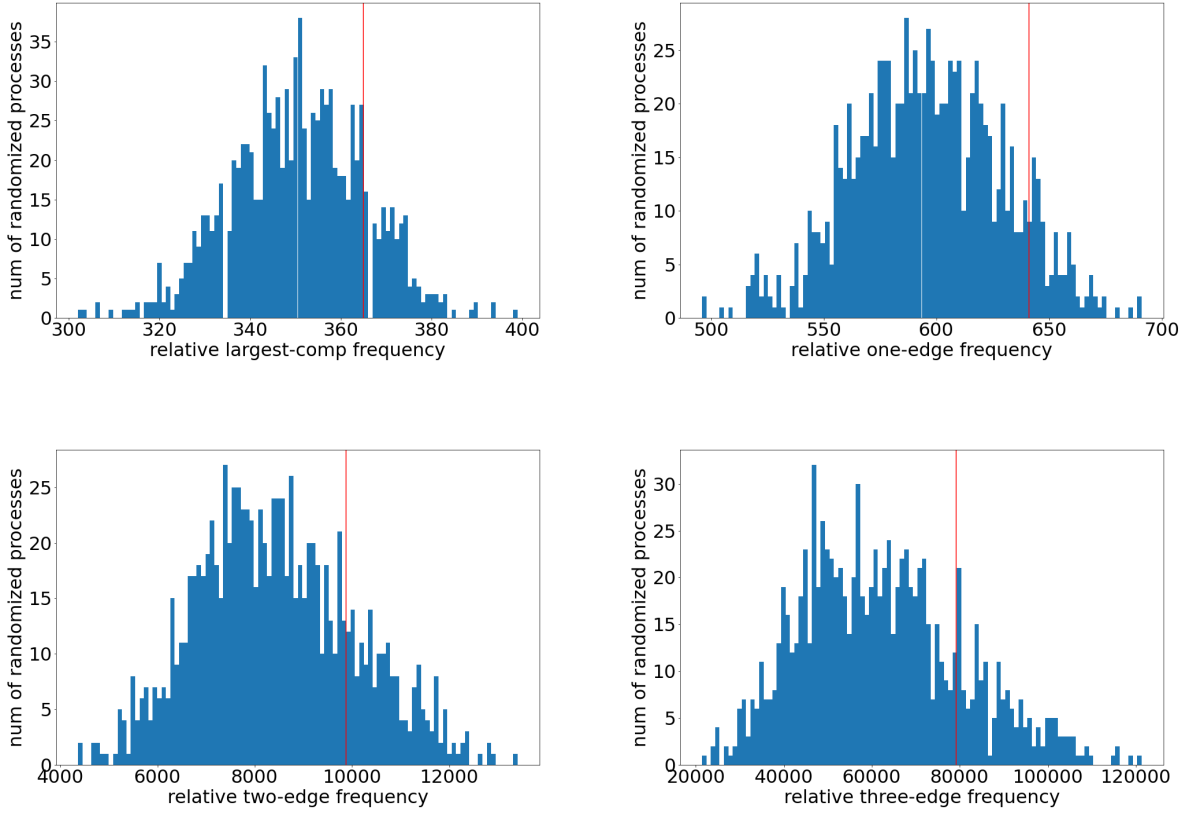


FIG. 10: Firm data Comparison of the real data statistic (red line) with the null distribution (blue), significance measured using p-value a) largest component $p = 0.175$ b) one-edge $p = 0.1$ c) two-edge $p = 0.203$ d) three-edge $p = 0.192$

the results are shown in Fig. 11

Results for the completely defaulted network are shown in the form of histograms in Fig 10, the red line represents the respective causal statistic count on the real process, and the blue histogram is the null distribution created by shuffling default times on network vertices. We chose the causal largest component and one, two and three-edge causal motifs as test statistics. According to the p-value, the most successful statistic is one-edge causal motif. Also the temporal evolution of the default process is shown in Fig. 11. Although one-edge causal motif is the best statistic when the complete network is defaulted, we can see that when between 70 and 90 percent of network three-edge causal motif prevails.

The results obtained in the simulations show that the three-edge statistic is most useful at smaller percentages (less than 50%) of default, while one-edge is best for completely defaulted networks. Applying these statistics on the real data we can conclude that an endogenous propagation of defaults was probably present.

VI. CONCLUSION

Our aim was, given a set of data, to be able to determine from it whether the explanation of observed process requires the endogenous network structure, or it is enough to model the dynamics as subject only to a field effect. We have developed a methodology which infers from the data represented as a temporal network whether there was an endogenous propagation of the default (contagion) or not.

We tested the methodology on synthetic data, and were able to distinguish if an endogenous component was present in the simulated process up to the value $\zeta = 1.0$, which represents a process with the endogenous rate with the same order of magnitude as the exogenous one. Using KS-test and z-score we were able to determine which test statistics is most suitable for which set of network and process parameters $(\langle k \rangle, \zeta)$ while considering all the motif classes univariate. We have done the same in the case of multivariate motifs and have shown using Mahalanobis distance that higher order motifs give more information about the process.

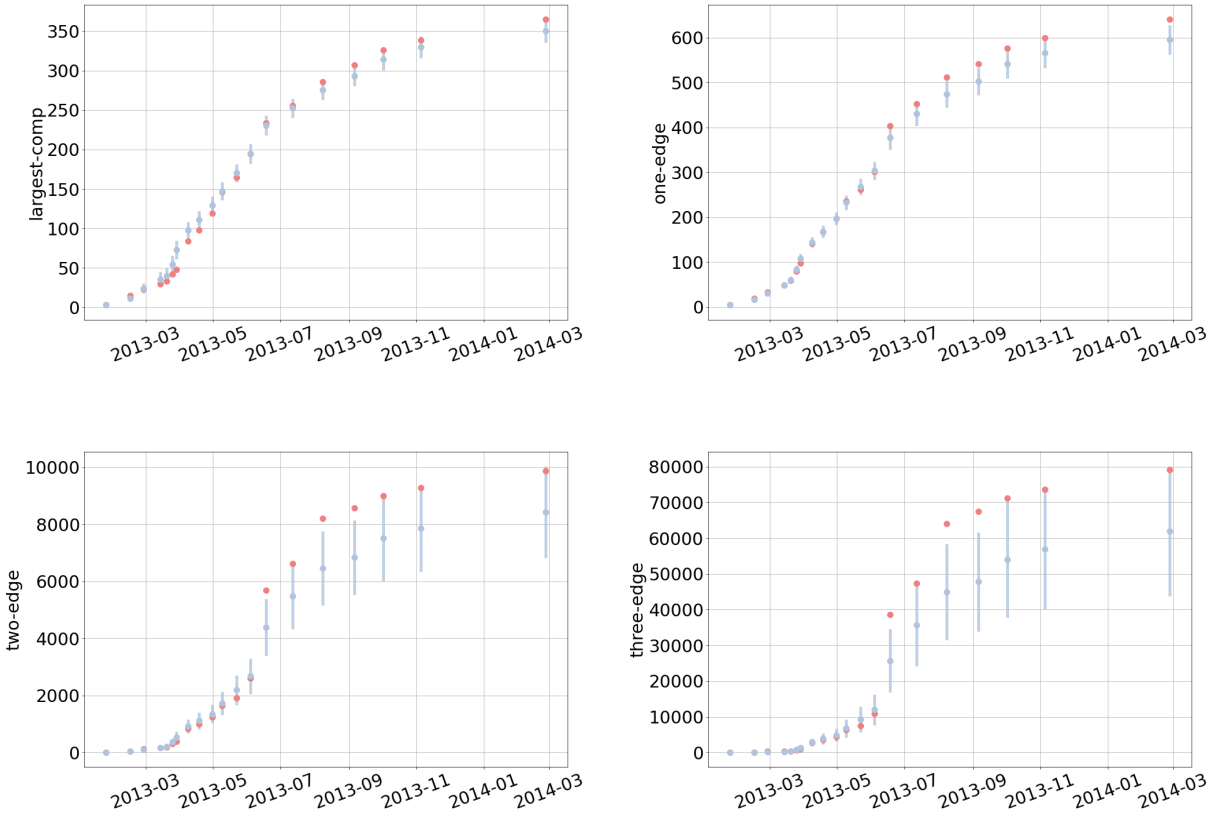


FIG. 11: Firm data Temporal evolution of the real data statistic (blue dot) with the null distribution standard deviation (blue) with $N = 1000$ randomisation.

In addition to providing a methodology, we extended the AME to directed networks with temporal ordering, and obtained the calculations for the simulated quantities.

Finally, we applied our method on the pre-bankruptcy settlement data of Croatian companies. Based on our analysis we can conclude that there *probably* was an endogenous propagation of defaults (prebankruptcy settlements) in the network, which is in agreement with previous research [25] which used a more extensive dataset including the values of debts, assets of companies etc. Here we demonstrated that we can distinguish an endogenous spreading even when using a minimal possible data set.

A natural extension for the future work with respect to economic cascades would be adding amounts of debt as weights on edges, as it is reasonable to assume that larger debts are more probable to serve for propagation of default than smaller debts. Also, the next refinement of the method could be a limit on the time that passes between the default of a debtor and the default of a creditor, since the probability that the debtor's default was the

cause of the creditor's default decays with time that passes. Systematic inclusion of more and more information to distinguish between mechanisms of endogenous propagation up to a point of purely data driven mechanisms is a research direction for which presented research is a good starting point.

In this paper we also did not enter into the question of different network classes like for instance correlated or scale-free networks [45]. Understanding the difference of detection in different classes would surely be of interest, especially since it is well known that they can have significant effects on contact processes [45, 49, 50].

Furthermore as is seen in this paper, sometime it is impossible to recognize if the endogenous process exist if the "noise" of exogenous process is too strong. There should exist a fundamental phase transition between detectable and undetectable phase of epidemics similar to community detection detectability limit [51]. This limit would be of great importance for the researchers interested in the exogenous - endogenous interplay of interacting particle systems on complex networks.

VII. ACKNOWLEDGMENTS

VZ and IB acknowledge partial support from QuantiXLie Centre of Excellence, a project co-financed by the Croatian Government and European Union through the European Regional Development Fund - the Competitiveness and Cohesion Operational Program (Grant KK.01.1.1.01.0004, element

leader N.P.). HS and VZ had their research supported by the European Regional Development Fund under the grant KK.01.1.1.01.0009 (DATACROSS). VZ also acknowledges the Croatian Science Foundation (HrZZ) Projects No. IP-2016-6-3347 and IP-2019-4-3321. Authors also want to express gratitude to Andrea Gabrielli and Ingo Scholtes for helpful discussions.

[1] R.M. Anderson, R.M. May, *Nature* **280**(5721), 361 (1979)

[2] R.M. Anderson, R.M. May, *Infectious diseases of humans: dynamics and control* (Oxford university press, 1992)

[3] I.Z. Kiss, J.C. Miller, P.L. Simon, et al., *Cham: Springer* **598** (2017)

[4] S. Battiston, M. Puliga, R. Kaushik, P. Tasca, G. Caldarelli, *Scientific reports* **2**, 541 (2012)

[5] P. Gai, S. Kapadia, *Proceedings of the Royal Society A: Mathematical, Physical and Engineering Sciences* **466**(2120), 2401 (2010)

[6] L. Weng, A. Flammini, A. Vespignani, F. Menczer, *Scientific reports* **2**, 335 (2012)

[7] D.G. Kendall, *The Annals of Mathematical Statistics* pp. 338–354 (1953)

[8] E. Volz, L.A. Meyers, *Proceedings of the Royal Society B: Biological Sciences* **274**(1628), 2925 (2007)

[9] S. Blower, M.H. Go, *BMC medicine* **9**(1), 1 (2011)

[10] I. Vodenska, A.P. Becker, in *New Perspectives and Challenges in Econophysics and Sociophysics* (Springer, 2019), pp. 101–116

[11] P.J. Mucha, T. Richardson, K. Macon, M.A. Porter, J.P. Onnela, *science* **328**(5980), 876 (2010)

[12] S. Boccaletti, G. Bianconi, R. Criado, C.I. Del Genio, J. Gómez-Gardenes, M. Romance, I. Sendina-Nadal, Z. Wang, M. Zanin, *Physics Reports* **544**(1), 1 (2014)

[13] E. Cozzo, G. Ferraz de Arruda, F. Aparecido Rodrigues, Y. Moreno, *Multiplex Networks*, 1st edn. SpringerBriefs in Complexity (Springer International Publishing, 2018)

[14] S. Battiston, D.D. Gatti, M. Gallegati, B. Greenwald, J.E. Stiglitz, *Journal of Financial Stability* **8**(3), 138 (2012)

[15] C.D. Brummitt, T. Kobayashi, *Physical Review E* **91**(6), 062813 (2015)

[16] V. Zlatić, G. Gabbi, H. Abraham, *PloS one* **10**(7), e0114928 (2015)

[17] T. Kobayashi, K. Hasui, *Scientific reports* **4**(1), 1 (2014)

[18] D.J. Watts, *Proceedings of the National Academy of Sciences* **99**(9), 5766 (2002)

[19] D. Acemoglu, A. Ozdaglar, A. Tahbaz-Salehi, *American Economic Review* **105**(2), 564 (2015)

[20] D. Acemoglu, V.M. Carvalho, A. Ozdaglar, A. Tahbaz-Salehi, *Econometrica* **80**(5), 1977 (2012)

[21] M.G. Hertzel, Z. Li, M.S. Officer, K.J. Rodgers, *Journal of Financial Economics* **87**(2), 374 (2008)

[22] E. Oberfield, *Econometrica* **86**(2), 559 (2018)

[23] J. Gao, The effects of firm network on banks' portfolio consideration. Tech. rep., Mimeo. Kelly School of Business, Indiana University (2015)

[24] L. Gauvin, M. Génois, M. Karsai, M. Kivelä, T. Takaguchi, E. Valdano, C.L. Vestergaard, arXiv preprint arXiv:1806.04032 (2018)

[25] S. Košćak, M. Šikić, H. Štefančić, M. Bešević Vlajo, V. Pribičević, V. Zlatić, *Hub Think Tank Broj 3: Arhitektura Mreže Dugovanja Hrvatskih Tvrđki* (2015). URL <https://www.hub.hr/hr/hub-think-tank-broj-3-architektura-mreze-dugovanja-hrvatskih-tvrđki>. (Text is in Croatian)

[26] M. Torricelli, M. Karsai, L. Gauvin, *Scientific Reports* **10**(1), 1 (2020)

[27] S. Lehmann, in *Temporal Network Theory* (Springer, 2019), pp. 25–48

[28] A. Mellor, arXiv preprint arXiv:1801.10527 (2018)

[29] R. Milo, S. Shen-Orr, S. Itzkovitz, N. Kashtan, D. Chklovskii, U. Alon, *Science* **298**(5594), 824 (2002)

[30] S.S. Shen-Orr, R. Milo, S. Mangan, U. Alon, *Nature genetics* **31**(1), 64 (2002)

[31] U. Alon, *Nature Reviews Genetics* **8**(6), 450 (2007)

[32] K. Ristl, S.J. Plitzko, B. Drossel, *Journal of theoretical biology* **354**, 54 (2014)

[33] T. Ohnishi, H. Takayasu, M. Takayasu, *Journal of Economic Interaction and Coordination* **5**(2), 171 (2010)

[34] F.W. Takes, W.A. Kosters, B. Witte, E.M. Heemskerk, *Applied network science* **3**(1), 39 (2018)

[35] V. Zlatić, M. Božićević, H. Štefančić, M. Domazet, *Physical Review E* **74**(1), 016115 (2006)

[36] A. Paranjape, A.R. Benson, J. Leskovec, in *Proceedings of the Tenth ACM International Conference on Web Search and Data Mining* (2017), pp. 601–610

[37] A. Anagnostopoulos, R. Kumar, M. Mahdian, in *Proceedings of the 14th ACM SIGKDD international conference on Knowledge discovery and data mining* (2008), pp. 7–15

[38] M. Piškorec, N. Antulov-Fantulin, I. Miholić, T. Šmuc, M. Šikić, in *International Conference on Complex Networks and their Applications* (Springer, 2017), pp. 1015–1027

[39] S.A. Myers, C. Zhu, J. Leskovec, in *Proceedings of the 18th ACM SIGKDD international conference on Knowledge discovery and data mining* (2012), pp. 33–41

[40] I. Barjašić, H. Štefančić, V. Pribičević, V. Zlatić, *Supplementary information*. URL https://github.com/ibarjasic94/default_process

[41] P.V. Paulau, C. Feenders, B. Blasius, *Scientific reports* **5**, 11926 (2015)

[42] A.C. Schwarze, M.A. Porter, arXiv preprint arXiv:2007.07447 (2020)

[43] T. LaRock, V. Nanumyan, I. Scholtes, G. Casiraghi, T. Eliassi-Rad, F. Schweitzer, in *Proceedings of the 2020 SIAM International Conference on Data Mining* (SIAM, 2020), pp. 460–468

[44] F.G. Elfadaly, P.H. Garthwaite, J.R. Crawford, *Computational statistics & data analysis* **99**, 115 (2016)

[45] M.E. Newman, A.L.E. Barabási, D.J. Watts, *The structure and dynamics of networks*. (Princeton university press, 2006)

[46] J.P. Gleeson, *Physical Review X* **3**(2) (2013). doi:10.1103/physrevx.3.021004. URL <http://dx.doi.org/10.1103/PhysRevX.3.021004>

[47] C. Matias, S. Schbath, E. Birmelé, J.J. Daudin, S. Robin, *REVSTAT-Statistical Journal* **4**(1), 31 (2006)

[48] R.T. Rust, C. Lee, E. Valente, *International Journal of Research in Marketing* **12**(4), 279 (1995). doi:[https://doi.org/10.1016/0167-8116\(95\)00014-0](https://doi.org/10.1016/0167-8116(95)00014-0). URL <http://www.sciencedirect.com/science/article/pii/0167811695000140>

[49] R. Pastor-Satorras, A. Vespignani, *Physical review letters* **86**(14), 3200 (2001)

[50] G. D'Agostino, A. Scala, V. Zlatić, G. Caldarelli, *EPL (Europhysics Letters)* **97**(6), 68006 (2012)

[51] R.R. Nadakuditi, M.E. Newman, *Physical review letters* **108**(18), 188701 (2012)